Supplemental Information

Initiation of the TORC1-Regulated G_0 Program Requires Igo1 and Igo2, which License Specific mRNAs to Bypass Degradation via the 5'-3' mRNA Decay Pathway

Nicolas Talarek, Elisabetta Cameroni, Malika Jaquenoud, Xuan Luo, Séverine Bontron, Soyeon Lippman, Geeta Devgan, Michael Snyder, James R. Broach, and Claudio De Virgilio

INVENTORY OF SUPPLEMENTAL INFORMATION

Supplemental Figures

Supplemental Tables

Supplemental Experimental Procedures

Supplemental References

Supplemental Figures

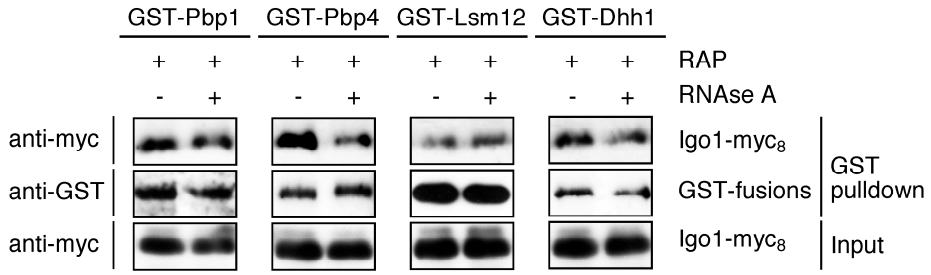

Figure S1. Associations of Igo1 with Pbp1, Pbp4, Lsm12, and Dhh1 are Insensitive to RNAse A Treatment

GST-Pbp1, GST-Pbp4, GST-Lsm12, GST-Dhh1, and GST were pulled down from lysates obtained from rapamycin-treated (+ RAP; 0.2 µg ml^{-1}; 2 hr) wild-type strains co-expressing Igo1-myc_8. Lysates were either treated (+) or not treated (-) with RNAse A prior to the pull-down experiments. Cell lysates and GST pulldown samples were subjected to SDS-PAGE and immunoblots were probed with anti-myc or anti-GST antibodies.

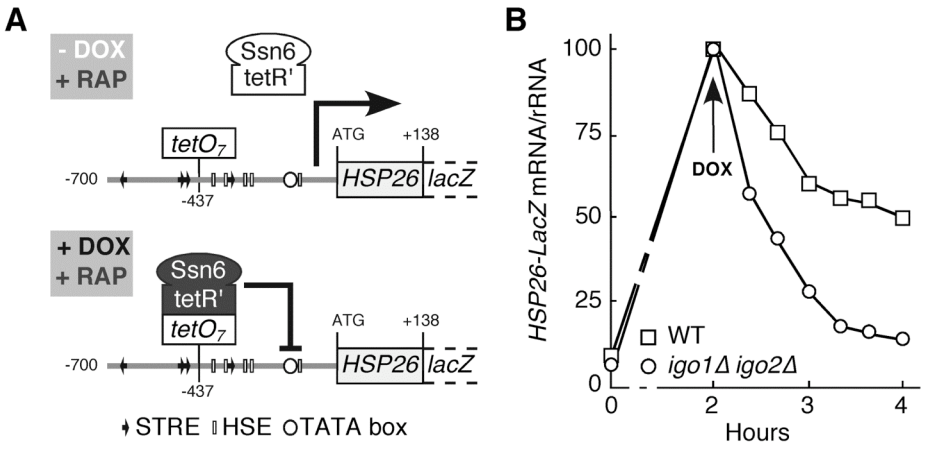

Figure S2. Igo1 and Igo2 Stabilize *HSP26-lacZ* mRNAs Following Inactivation of TORC1

(A) Schematic view of the *HSP26-lacZ* reporter gene (used in B) illustrating 700 nucleotides of the *HSP26* promoter region including the positions of the stress-response elements (STREs), the heat-shock-elements (HSEs; Chen and Pederson, 1993), and the inserted seven doxycycline-responsive *tetO* elements (*$tetO_7$*). Nucleotide +138 of *HSP26* is fused to the *lacZ* gene. Doxycycline treatment triggers binding of the chimeric tetR'-Ssn6 fusion protein to the *$tetO_7$* region and consequently mediates transcriptional repression of the reporter gene.

(B) Exponentially growing wild-type (□) and *igo1*Δ *igo2*Δ (○) cells harboring the doxycycline-repressible reporter and expressing the chimeric tetR'-Ssn6 protein were treated with rapamycin (0.2 µg ml^{-1}) at time 0. After 2 hr, cells were treated with doxycycline (DOX; 15 µg ml^{-1}) and grown for additional 2 hr in the continuous presence of rapamycin. *HSP26-lacZ* transcript levels were determined via northern blot analysis, quantified by PhosphorImager analysis, and expressed as relative level of *HSP26-lacZ* mRNA per rRNA (arbitrarily set to 100% for both strains for the values at the 2 hr time point of the rapamycin treatment; the relative *HSP26-lacZ* transcript levels were 3-fold higher in wild-type than in *igo1*Δ *igo2*Δ cells at this time point). In control experiments, addition of doxycycline prior to the rapamycin treatment fully abolished the *HSP26-lacZ* induction in wild-type and *igo1*Δ *igo2*Δ cells (not shown). The calculated half live of the *HSP26-lacZ* mRNA was 104 min (± 7 SD; n = 3) and 36 min (± 4 SD; n = 3) in rapamycin-treated wild-type and *igo1*Δ *igo2*Δ cells, respectively.

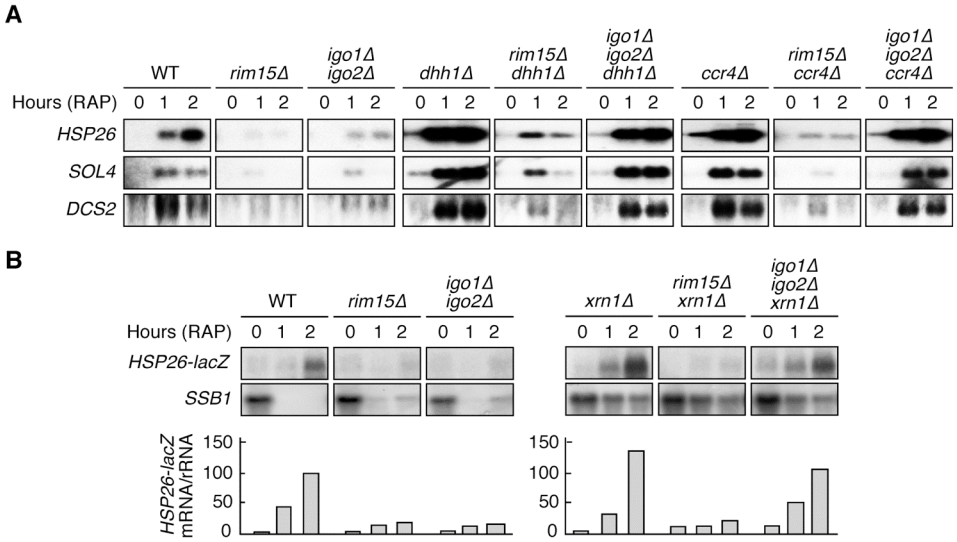

Figure S3. The 5'-3' mRNA Decay Pathway Targets Specific mRNAs in *igo1*Δ *igo2*Δ Mutants

(A) Loss of Dhh1 or Ccr4 suppresses the defect of *igo1*Δ *igo2*Δ, but not that of *rim15*Δ cells, in rapamycin-induced *HSP26*, *SOL4*, and *DCS2* mRNA expression. Transcript levels were determined by northern blot analysis in wild-type (WT) and mutant strains prior to (0) and following a 1-hr or 2-hr rapamycin treatment (RAP; 0.2 μg ml^{-1}).

(B) *HSP26-LacZ* transcript levels prior to and following rapamycin treatment. Transcript levels of *HSP26-lacZ* and *SSB1* were determined by northern blot analysis in wild-type (WT) and indicated mutant strains prior to (0) and following a rapamycin treatment (RAP; 0.2 μg ml^{-1}) of 1 hr or 2 hr. Bar graphs show the relative level of *HSP26-lacZ* mRNA per rRNA (arbitrarily set to 1.0 for exponentially growing wild-type cells).

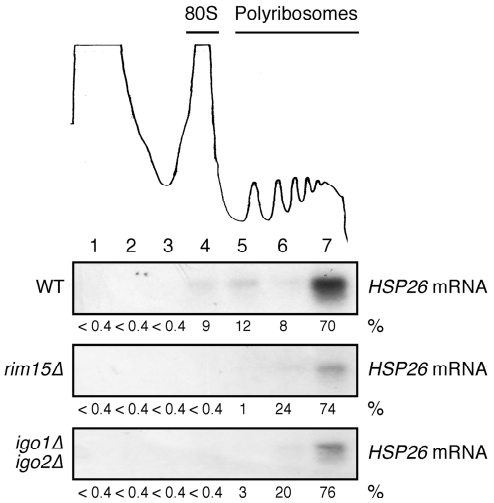

Figure S4. *HSP26* mRNA Fractionates with Polyribosomes on Sucrose Gradients in the Absence of Igo1/2

The top trace shows the UV absorbance profile at 254 nm of a cell extract of rapamycin-treated (2 hr; 0.2 μg ml^{-1}) wild-type yeast after sedimentation on a 7 to 50 % linear sucrose gradient. Nearly identical profiles were obtained from *rim15*Δ and *igo1*Δ *igo2*Δ cell extracts (not shown). Aligned below are northern blots performed on total RNA isolated from the indicated (1-7) sucrose gradient fractions of wild-type (WT), *rim15*Δ, and *igo1*Δ *igo2*Δ cell extracts (all harvested after a 2-hr rapamycin treatment). The relative levels of *HSP26* input mRNA (set to 100% for wild-type cells) were 18% and 32% for *rim15*Δ and *igo1*Δ *igo2*Δ cells, respectively. The positions of the 80S monosomes and polyribosomes are indicated. *HSP26* mRNA was quantified by PhosphorImager analysis and the percentage of *HSP26* mRNA in the indicated sucrose gradient fractions is indicated at the bottom of each panel.

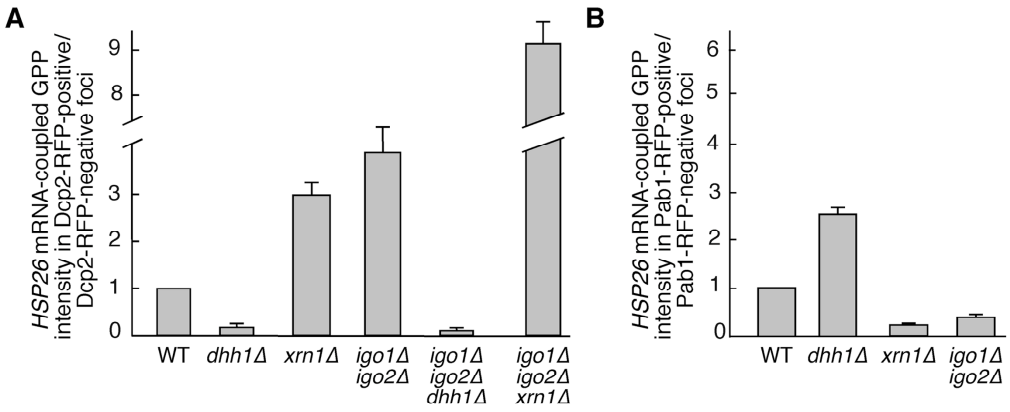

Figure S5. Relative Distribution of *HSP26* mRNAs Among Cytoplasmic Foci

(A, B) Wild-type (WT) and indicated mutant strains co-expressing the PB-marker protein Dcp2-RFP (A) or the EGPB/SG-marker protein Pab1-RFP (B), as well as *HSP26-U1A* mRNA and the U1A-GFP binding protein were harvested following glucose limitation (*i.e.* following growth for 48 hr in batch cultures). Bars represent (in a total of 100 cells) the ratio between the intensity of *HSP26* mRNA-coupled GFP signal in cytoplasmic foci that co-stained with Dcp2-RFP (A) or Pab1-RFP (B) and that detected in foci devoid of the corresponding RFP signal. This ratio was set to 1.0 for wild-type cells. Data represent averages (n = 3), with SDs indicated by the lines above each bar. The GFP signal in each *HSP26* mRNA-containing cytoplasmic focus was calculated as the mean intensity within the region of the focus multiplied by its area, after subtraction of the mean background intensity of a nearby area of comparable size. Within an experiment, exposure settings were identical. Notably, loss of Xrn1, like loss of Igo1/2, strongly shifted the relative distribution of *HSP26* mRNAs among cytoplasmic foci towards Dcp2-RFP-positive PBs and the effects of loss of both Igo1/2 and of Xrn1 appeared to be additive (A). As expected, loss of Dhh1 enhanced, while loss of Xrn1 or of Igo1/2 reduced, the relative amount of *HSP26* mRNAs in Pab1-RFP-positive EGPBs/SGs (B).

Supplemental Tables

Table 1. Strains Used in This Study

Strain	Genotype	Source	Figure/Table
BY4741	MATa; *his3Δ1, leu2Δ0, met15Δ0, ura3Δ0*	Euroscarf	1B, E, F, 2A, C, D, 4, 5A-C, 6A-D, S3, S4, S5A, Table3
BY4742	MATα; *his3Δ1, leu2Δ0, lys2Δ0, ura3Δ0*	Euroscarf	
YFL033C	MATa*; rim15Δ::kanMX4* [BY4741]	Euroscarf	1E, F, 2A, C, D, 5A-C, 6B-D, S3, S4
YNL157W	MATa*; igo1Δ::kanMX4* [BY4741]	Euroscarf	2A, C, D, 3B, 7A, C, S1
YHR132W-A	MATa*; igo2Δ::kanMX4* [BY4741]	Euroscarf	2A, C, D
CDV288-12A	MATa*; igo1Δ::kanMX4, igo2Δ::kanMX4* [BY4741]	This study	2A, C, D, 4, 5A-C, 6B-D, S3, S4, S5A
LC54	MATa*; IGO1-myc$_{13}$::kanMX4* [BY4741]	This study	3A, Table 3
MJA1709-8B	MATa*; rim15Δ::kanMX4 IGO1-myc$_{13}$::kanMX4* [BY4741]	This study	3A
NT255-1B	MATa*; leu2Δ0::LEU2-TetR'-SSN6* [BY4741/2]	This study	S2B
NT280-12D	MATa*; leu2Δ0::LEU2-TetR'-SSN6 igo1Δ::kanMX4, igo2Δ::kanMX4* [BY4741/2]	This study	S2B
YDL160C	MATa*; dhh1Δ::kanMX4* [BY4741]	Eursocarf	5A-C, S3A, S5A
YAL021C	MATa*; ccr4Δ::kanMX4* [BY4741]	Euroscarf	5A-C, S3A
NT205-1B	MATa*; xrn1Δ::kanMX4* [BY4741/2]	This study	5A-C, 6B-D, S3B, S5A
MJA1602-3A	MATα*; rim15Δ::kanMX4, dhh1Δ::kanMX4* [BY4741/2]	This study	5A-C, S3A
MJA1600-10B	MATα*; rim15Δ::kanMX4, ccr4Δ::kanMX4* [BY4741/2]	This study	5A-C, S3A
MJA1621-10B	MATa*; igo1Δ::kanMX4, igo2Δ::kanMX4, dhh1Δ::kanMX4* [BY4741/2]	This study	5A-C, S3A, S5A
MJA1597-4D	MATa*; igo1Δ::kanMX4, igo2Δ::kanMX4, ccr4Δ::kanMX4* [BY4741/2]	This study	5A-C, S3A
NT205-1A	MATa*; rim15Δ::kanMX4, xrn1Δ::kanMX4* [BY4741/2]	This study	5A-C, 6B-D, S3B
NT206-7A	MATa*; igo1Δ::kanMX4, igo2Δ::kanMX4, xrn1Δ::kanMX4* [BY4741/2]	This study	5A-C, 6B-D, S3B, S5A
Y2864	MATα; *gal1Δ::HIS3, ade2-1, his3-11,15, leu2-3,112, trp1-1, ura3-1, can1-100*	Wang *et al.*, 2004	2B
CDV314	MATα; *rim15Δ::kanMX4* [Y2864]	This study	2B
CDV308-1B	MATα*; igo1Δ::kanMX4, igo2Δ::kanMX4* [Y2864]	This study	2B
yMK1344	MATα, *his3-11, 15, leu2-3, 112, trp1-1, ura3-1, DCP1-GFP::G418, PAB1-RFP::NAT*	Hoyle et al., 2007	
NT253-13B	MATα; *igo1Δ::kanMX4, PAB1-RFP::NAT* [BY4741/2]	This study	7B
NT169-9C	MATa; *PAB1-RFP::NAT* [BY4741/2]	This study	7D, S5B
NT255-6B	MATa; *igo1Δ::kanMX4, igo2Δ::kanMX4, PAB1-RFP::NAT* [BY4741/2]	This study	S5B
NT298	MATa; *dhh1Δ::kanMX4, PAB1-RFP::NAT* [BY4741/2]	This study	S5B
NT301	MATa; *xrn1Δ::kanMX4, PAB1-RFP::NAT* [BY4741/2]	This study	S5B

Table 2. Plasmids Used in This Study

Plasmid	Description	Source	Figure/Table
YEplac181	2μ, *LEU2*	Gietz and Sugino, 1988	
pCDV1157	[YEPlac181] *TDH3p-IGO1-HA$_3$*	This study	1B
pCDV1159	[YEPlac181] *TDH3p-SIR4-HA$_3$*	This study	1B
YEplac195	2μ, *URA3*	Gietz and Sugino, 1988	
pNB566	[YEPlac195] *GAL1p-GST-RIM15*	Wanke *et al.*, 2005	1B
pLC803	[YEPlac195] *GAL1p-GST*	This study	1B
pCDV487	[YEPlac195] *GAL1p-GST-RIM15-HA$_3$*	Pedruzzi *et al.*, 2003	1B,C, D
pIP779	[YEPlac195] *GAL1p-GST-RIM15^{K823Y}-HA$_3$*	This study	1C, D
pGEX3	*GST*	Smith and Johnson,1988	1C
pLC1092	[pGEX3] *GST-IGO1*	This study	1C, D
pLC1134	[pGEX3] *GST-IGO1^{S64A}*	This study	1C
pVW1109	[pGEX3] *GST-IGO2*	This study	1C
MJA1497	[pGEX3] *GST-ENSA*	This study	1C
MJA1498	[pGEX3] *GST-ARPP-19*	This study	1C
YCplac33	CEN, *URA3*	Gietz and Sugino, 1988	2D
pBG1805-IGO1-TAP	*GAL1p-IGO1-HA-6HIS-3C-ZZ*	Gelperin et al., 2005	Table 3
pLC1427	[YCplac33] *IGO1-myc$_8$*	This study	2D, 3B, S1
pLC1430	[YCplac33] *IGO1^{S64A}-myc$_8$*	This study	2D, 3B
pLC1429	[YCplac33] *IGO2-myc$_8$*	This study	2D
pMJA1481	[YEplac195] *IGO1p-ENSA-myc$_8$*	This study	2D
pMJA1482	[YEplac195] *IGO1p-ARPP-19-myc$_8$*	This study	2D
pUKC414	CEN, *URA3, HSP26-lacZ*	Ferreira *et al.*, 2001	5C, 6C
pXL1633	CEN, *HIS3, HSP26-lacZ*	This study	2D
pCDV1082	YCpIF2-*ADH1p-GST*	This study	3A, B, S1
pMJA1655	YCpIF2-*ADH1p-GST-PBP4*	This study	3A, B, S1
pMJA1654	YCpIF2-*ADH1p-GST-PBP1*	This study	3A, B, S1
pMJA1656	YCpIF2-*ADH1p-GST-DHH1*	This study	3A, B, S1
pMJA1657	YCpIF2-*ADH1p-GST-LSM12*	This study	3A, B, S1
pCM242	CMVp*(tetR'-SSN6)::LEU2*	Belli et al., 1998	S2B
pNT012	CEN, URA3, *HSP26p::tetO$_7$-HSP26-LacZ*	This study	S2A, B
pTG003	PRS315-*DCP2-RFP*	Gill et al., 2006	6A, D, 7A, S5A
pPS2037	PRS416-*PGK1p-PGK1-U1A-PGK1* 3'UTR	Brodsky and Silver, 2000	
pNT003	PRS416-*HSP26p-HSP26-U1A-HSP26* 3'UTR	This study	6A, D, 7C, D, S5
pPS2045	PRS313-*GALp-U1A*(1-94)-*GFP*	Brodsky and Silver, 2000	
pNT004	PRS413-*ADH1p-U1A*(1-94)-*GFP*	This study	6A, D, 7C, D, S5
pXL1632	[YCplac33] *IGO1-GFP*	This study	7A, B
pNT005	[YCplac33] *IGO1-RFP*	This study	7C

Table 3. Proteins Identified in Igo1-TAP and Igo1-myc$_{13}$ Pull-Down Experiments

Protein[1]	Igo1-TAP	Igo1-myc$_{13}$	MW	Function/Description
Act1		✓	41.7	Actin
Ate1	✓		57.9	Arginyl-tRNA-protein transferase
Clu1	✓		145.2	Component of eIF3
Hhf1/2		✓	11.4	Histone H4
Hrk1	✓		85.7	Protein kinase implicated in activation of Pma1
Hsc82		✓	80.9	Cytoplasmic chaperone of the Hsp90 family
Htb1		✓	14.3	Histone H2B
Igo1	✓	✓	18.0	Required for initiation of G_0; target of Rim15 protein kinase
Ilv6	✓		34.0	Regulatory subunit of acetolactate synthase
Lsm12	✓	✓	21.3	Sm-like protein; interacts with Pbp1/4; associates with ribosomes
Mot2	✓		65.4	Subunit of the CCR4-NOT complex
Pbp1	✓	✓	78.8	Interacts with Pab1 to regulate mRNA polyadenylation
Pbp4	✓	✓	19.9	Pbp1p binding protein 4; interacts with Lsm12
Por1		✓	30.4	Mitochondrial porin, outer membrane protein
Psp2	✓		65.6	Possible role in mitochondrial mRNA splicing
Rim1		✓	15.4	Role in mitochondrial DNA replication; binds single-stranded DNA
Rps18A		✓	17.0	Protein component of the small (40S) ribosomal subunit
Rsp5	✓		91.8	E3 ubiquitin-protein ligase
Sec23	✓		85.4	GTPase-activating protein; involved in ER to Golgi transport
Sfp1	✓		74.8	Transcription factor controlling expression of Ribi genes
Ssa1/2	✓	✓	69.6	Hsp70 family member
Ssa4		✓	69.7	Hsp70 family member
Ssb1/2	✓	✓	66.6	Hsp70 family member; ribosome-associated molecular chaperone
Ssc1	✓		70.6	Hsp70 family member; role in mitochondrial protein import
Tef1		✓	50.0	Translational elongation factor EF-1α

[1]Proteins were identified by LC-MS-MS analysis of polypeptides in purified Igo1-TAP and Igo1-myc$_{13}$ preparations (see Experimental Procedures). Only proteins for which at least four peptides were identified and, in the case of Igo1-TAP, for which the number of identified peptides was also at least four times higher than the number of peptides recovered with an unrelated control (Gtr1-TAP) were included in the list. The preparations (*i.e.* Igo1-TAP and/or Igo1-myc$_{13}$) in which corresponding peptides were identified are indicated (✓). Proteins for which peptides were recovered in both Igo1-TAP and Igo1-myc$_{13}$ preparations are highlighted in bold.

Supplemental Experimental Procedures

Proteome Chip Analyses

Yeast proteome microarrays were prepared as previously described (Ptacek et al., 2005). Approximately 4400 GST::His-tagged yeast proteins were overexpressed and purified by affinity chromatography and spotted in duplicate on a surface-modified microscope slide. The autophosphorylating kinases Pka2, Pkc-a and Cmk1 were added at defined locations to serve as both positive controls and landmarks for the identification of phosphorylation signals on the array. Common kinase substrates, such as myelin basic protein (MBP), histone H1, casein, polyGlu-Tyr, and a carboxyterminal domain (CTD) peptide containing three copies of the acidic CTD of RNA polymerase II were also included to exhibit the addition of kinase activity on the array.

To determine the optimal amount of kinase to use for probing the proteome arrays, a dilution series (1:1, 1:2, 1:5, 1:10, and 1:20) of wild-type Rim15 and kinase-inactive $Rim15^{KD}$ was made in a total volume of 200 µl kinase buffer containing 2 µl [γ-^{33}P] ATP and added to test arrays containing positive controls and common kinase substrates as described (Ptacek et al., 2005). Using the optimized conditions, proteome arrays were probed in duplicate with wild-type Rim15 and $Rim15^{KD}$ in 200 µl kinase buffer containing 2 µl [γ-^{33}P]ATP in a humidified chamber at 30°C for 1 hr. Arrays were then exposed to X-ray film for 1, 3 and 7 days. Data analysis was performed as described previously (Ptacek et al., 2005). In short, substrate proteins that displayed reproducible signals higher than those of neighboring spots in at least three of the four spots were identified and then compared to the autophosphorylation control. Only those spots that were specifically phosphorylated in the presence of wild-type Rim15 were scored as positive substrates. The proteome arrays probed with $Rim15^{KD}$ exhibited signals identical to those obtained in the absence of protein kinase.

Polysome Analyses

Strains were grown in synthetic defined medium to mid-log phase and either treated, or not, with rapamycin for 2 hr. Cycloheximide (0.1 mg ml^{-1} final concentration) was added just prior to harvesting. Extracts (of 150 OD_{600} of yeast cultures) were layered onto 7-50% linear sucrose gradients and centrifuged at 35'000 rpm at 4°C for 210 min. Gradient analysis was performed using an ISCO UA-6 collector with continuous monitoring at A_{254nm}. Manually collected fractions were used for RNA extraction as described (Gaillard and Aguilera, 2008).

Supplemental References

Belli, G., Gari, E., Piedrafita, L., Aldea, M., and Herrero, E. (1998). An activator/repressor dual system allows tight tetracycline-regulated gene expression in budding yeast. Nucleic. Acids Res. *26*, 942-947.

Brodsky, A.S., and Silver, P.A. (2000). Pre-mRNA processing factors are required for nuclear export. RNA *6*, 1737-1749.

Chen, J., and Pederson, D.S. (1993). A distal heat shock element promotes the rapid response to heat shock of the *HSP26* gene in the yeast *Saccharomyces cerevisiae*. J. Biol. Chem. *268*, 7442-7448.

Ferreira, P.C., Ness, F., Edwards, S.R., Cox, B.S., and Tuite, M.F. (2001). The elimination of the yeast [*PSI*$^+$] prion by guanidine hydrochloride is the result of Hsp104 inactivation. Mol. Microbiol. *40*, 1357-1369.

Gaillard, H., and Aguilera, A. (2008). A novel class of mRNA-containing cytoplasmic granules are produced in response to UV-irradiation. Mol. Biol. Cell *19*, 4980-4992.

Gietz, R.D., and Sugino, A. (1988). New yeast-*Escherichia coli* shuttle vectors constructed with *in vitro* mutagenized yeast genes lacking six-base pair restriction sites. Gene *74*, 527-534.

Gill, T., Aulds, J., and Schmitt, M.E. (2006). A specialized processing body that is temporally and asymmetrically regulated during the cell cycle in *Saccharomyces cerevisiae*. J. Cell Biol. *173*, 35-45.

Hoyle, N.P., Castelli, L.M., Campbell, S.G., Holmes, L.E., and Ashe, M.P. (2007). Stress-dependent relocalization of translationally primed mRNPs to cytoplasmic granules that are kinetically and spatially distinct from P-bodies. J. Cell Biol. *179*, 65-74.

Pedruzzi, I., Dubouloz, F., Cameroni, E., Wanke, V., Roosen, J., Winderickx, J., and De Virgilio, C. (2003). TOR and PKA signaling pathways converge on the protein kinase Rim15 to control entry into G_0. Mol. Cell *12*, 1607-1613.

Ptacek, J., Devgan, G., Michaud, G., Zhu, H., Zhu, X., Fasolo, J., Guo, H., Jona, G., Breitkreutz, A., Sopko, R., et al. (2005). Global analysis of protein phosphorylation in yeast. Nature *438*, 679-684.

Smith, D.B., and Johnson, K.S. (1988). Single-step purification of polypeptides expressed in *Escherichia coli* as fusions with glutathione *S*-transferase. Gene *67*, 31–40.

Wang, Y., Pierce, M., Schneper, L., Guldal, C.G., Zhang, X., Tavazoie, S., and Broach, J.R. (2004). Ras and Gpa2 mediate one branch of a redundant glucose signaling pathway in yeast. PLoS Biol. *2*, E128.

Wanke, V., Pedruzzi, I., Cameroni, E., Dubouloz, F., and De Virgilio, C. (2005). Regulation of G_0 entry by the Pho80-Pho85 cyclin-CDK complex. EMBO J. *24*, 4271-4278.